Meteoritics & Planetary Science 41, Nr 1, 125–133 (2006)
Abstract available online at http://meteoritics.org

Shock, post-shock annealing, and post-annealing shock in ureilites

Alan E. RUBIN*

Institute of Geophysics and Planetary Physics, University of California—Los Angeles, California 90095–1567, USA
*Corresponding author. E-mail: aerubin@ucla.edu

(Received 02 May 2005; revision accepted 09 August 2005)

Abstract–The thermal and shock histories of ureilites can be divided into four periods: 1) formation, 2) initial shock, 3) post-shock annealing, and 4) post-annealing shock. Period 1 occurred ~4.55 Ga ago when ureilites formed by melting chondritic material. Impact events during period 2 caused silicate darkening, undulose to mosaic extinction in olivines, and the formation of diamond, lonsdaleite, and chaoite from indigenous carbonaceous material. Alkali-rich fine-grained silicates may have been introduced by impact injection into ureilites during this period. About 57% of the ureilites were unchanged after period 2. During period 3 events, impact-induced annealing caused previously mosaicized olivine grains to become aggregates of small unstrained crystals. Some ureilites experienced reduction as FeO at the edges of olivine grains reacted with C from the matrix. Annealing may also be responsible for coarsening of graphite in a few ureilites, forming euhedral-appearing, idioblastic crystals. Orthopyroxene in Meteorite Hills (MET) 78008 may have formed from pigeonite by annealing during this period. The Rb-Sr internal isochron age of ~4.0 Ga for MET 78008 probably dates the annealing event. At this late date, impacts are the only viable heat source. About 36% of ureilites experienced period 3 events, but remained unchanged afterwards. During period 4, ~7% of the ureilites were shocked again, as is evident in the polymict breccia, Elephant Moraine (EET) 83309. This rock contains annealed mosaicized olivine aggregates composed of small individual olivine crystals that exhibit undulose extinction.

Ureilites may have formed by impact-melting chondritic material on a primitive body with heterogeneous O isotopes. Plagioclase was preferentially lost from the system due to its low impedance to shock compression. Brief melting and rapid burial minimized the escape of planetary-type noble gases from the ureilitic melts. Incomplete separation of metal from silicates during impact melting left ureilites with relatively high concentrations of trace siderophile elements.

INTRODUCTION

Ureilites are the second most abundant achondrite group (after HED), comprising ~100 specimens (Hutchison 2004). The group is enigmatic, as it appears to manifest primitive characteristics (e.g., planetary-type noble gases, heterogeneous O isotopes, and high concentrations of trace siderophile elements) as well as evolved, igneous characteristics (e.g., non-chondritic mineralogy, low concentrations of volatile elements, fractionated REE patterns, high Ca/Al ratios, and petrofabrics). The diverse models of ureilite formation reflect this dichotomy (Goodrich 1992). Primitive models include formation by planetesimal-scale collisions (Takeda 1987; Takeda et al. 1988), nebular sedimentation processes that form a plagioclase-depleted parent body (Takeda and Yanai 1978; Takeda et al. 1980; Takeda 1989) and impact-melting of material near the surface of a CV-like asteroid (Rubin 1988). Evolved models include formation from multi-stage igneous cumulates (Goodrich et al. 1987), partially disruptive impacts (Warren and Kallemeyn 1989), and explosive volcanism (Scott et al. 1993; Warren and Kallemeyn 1992).

There is no dispute that ureilites experienced high temperatures: it is clear that melt was involved in the formation of their coarse (≥1 mm) olivine and pyroxene grains (e.g., Fig. 4 of Berkley 1986). The 120° triple junctures at olivine and pyroxene grain boundaries that define the textures of many ureilites (e.g., Fig. 1a of Berkley et al. 1980; Fig. 1a of Goodrich 1992) indicate a high degree of textural equilibrium. It is also clear that ureilites were significantly shocked: many contain diamonds (Lipschutz 1964) and most exhibit silicate darkening (see below). Elucidation of the details of the thermal and shock histories of ureilites can help constrain the origin of these peculiar rocks.

Table 1. Ureilites examined in this study.

Meteorite	Section	Highest period reached
ALH 77257	99	3
ALH 78019	13	3
ALH 78262	19	2
ALH 81101	28	3
ALH 84136	22	3
CMS 04048	7	2
EET 83309	14	4
EET 87720	12	3
EET 90019	11	2
EET 96001	7	2
EET 96322	7	2
GRA 95205	12	3
HH 126[a]	UCLA 1842	2
Hughes 009	AMNH 4814-3	2
Kenna	UCLA 1859	2
LAP 03587	7	2
LAR 04315	20; 21	4
LEW 86216	4	3
MET 78008	32	3
NWA 1006	UCLA 1857	2
NWA 1241	UCLA 1843	2
NWA 1462	UCLA 1844	2
NWA 1464	UCLA 1845	2
NWA 2225	UCLA 1858	2
Nova 001	S1686	3
PCA 82506	67	2
RKP 80239	10	2
Reid 016	AMNH 4882-1	3

[a]HH 126 = Hammadah al Hamra 126.

Antarctic sections are from NASA-Johnson Space Center; AMNH = American Museum of Natural History; Section S1686 of Nova 001 is from Allan Treiman of the Lunar and Planetary Institute.

ANALYTICAL PROCEDURES

I examined thin sections of a suite of 28 ureilites microscopically (Table 1). Apparent grain sizes were measured using a calibrated reticle. The compositions of olivine grains in Allan Hills (ALH) 77257 were determined with the JEOL JXA-8200 electron microprobe at the University of California—Los Angeles using a focused beam, natural and synthetic standards, an accelerating voltage of 15 keV, a 15 nA sample current, 20 sec counting times per element, and ZAF corrections. Backscattered electron (BSE) images of ALH 77257 were also made with the UCLA JEOL probe.

RESULTS AND DISCUSSION

The petrogenetic histories of ureilites can be divided into four periods: 1) formation, 2) initial shock, 3) post-shock annealing, and 4) post-annealing shock. During each period, ureilites were subjected to a number of events that affected their bulk properties.

Period 1: Formation

Ureilites contain coarse (millimeter-size) olivine and pyroxene grains (Fig. 1) that either crystallized from or equilibrated with melts at high temperatures. Cohenite [$(Fe,Ni)_3C$] is present inside metallic spherules that occur within olivine and pigeonite grains in several ureilites (Goodrich and Berkley 1986), indicating that the melts from which ureilites formed were carbon-rich. This is consistent with the correlation in ureilites between $\Delta^{17}O$ and wt% C (Clayton and Mayeda 1988) that demonstrates that C was indigenous to the ureilite parent body. Interstitial carbonaceous material that occurs along olivine and pyroxene grain boundaries (e.g., Fig. 1 of Berkley et al. 1980) is probably a primary feature. The strong preferential orientation of elongated mafic minerals in ureilites (e.g., Fig. 1 of Berkley et al. 1976) is either a primary feature caused by the accumulation of grains at the base of a crystallizing melt or a late-stage shock feature akin to those that deformed reduced CV chondrites, ordinary chondrites, and CR chondrites (e.g., Cain et al. 1986; Sneyd et al. 1988; Weisberg et al. 1993).

The Sm-Nd whole-rock ages of several ureilites (Allan Hills [ALH] 82130, Meteorite Hills [MET] 78008, and Pecora Escarpment [PCA] 82506) are consistent with a 4.55 Ga chondritic isochron (Goodrich 1992), suggesting that this date represents the formation age of ureilites. The Rb-Sr model age of MET 78008 is also 4.55 Ga (Takahashi and Matsuda 1990). Those ureilites with younger Sm-Nd isochron ages (e.g., some portions of PCA 82506 at 4.23 Ga; Kenna and Novo Urei at 3.74 Ga) may have suffered isotopic disturbance, probably by episodes of impact heating.

Period 2: Initial Shock

All ureilites manifest a variety of shock effects, which indicates that they all experienced period 2 events. Despite Goodrich's (1992) characterization of some ureilites as having a low shock state, all ureilites seem to have reached shock stage S2, S3, or beyond (cf. Stöffler et al. 1991).

Silicate darkening is present in all ureilites in this study (e.g., Fig. 2). It is caused by the dispersion within silicate grains of 10–500 μm long curvilinear trails composed of 0.2–4 μm blebs of metallic Fe-Ni and accessory sulfide. Although Singletary and Grove (2003) reported trails of tiny metal inclusions only in pigeonite grains in ureilites, these trails also occur in olivine. For example, Fig. 2 shows an olivine grain (Fa 13.8) in ALH 77257 that contains numerous small opaque inclusions. The edge of the grain (the left side of the image) is a reduction rim containing thousands of tiny low-Ni metallic Fe blebs formed from FeO in the olivine by reduction (see below). Some curvilinear trails of metallic Fe blebs in the grain (e.g., the right side of Fig. 2) are flanked by dark-shaded, relatively low-FeO

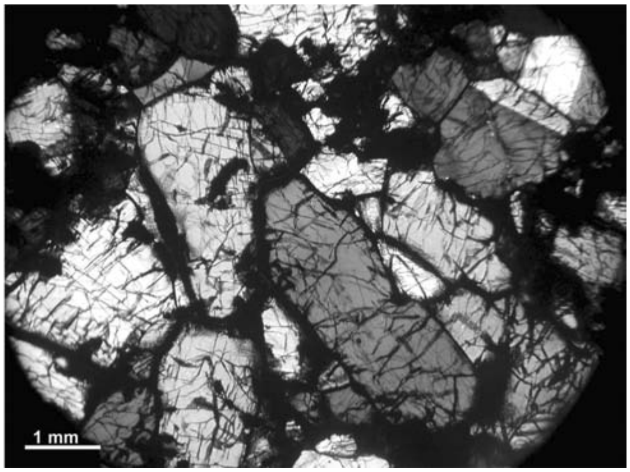

Fig. 1. Typical ureilite texture in ALH 77257 consisting of coarse olivine and pyroxene grains (light gray) with interstitial carbonaceous material (black). Many silicate grain boundaries form 120° triple junctions. X-nicols.

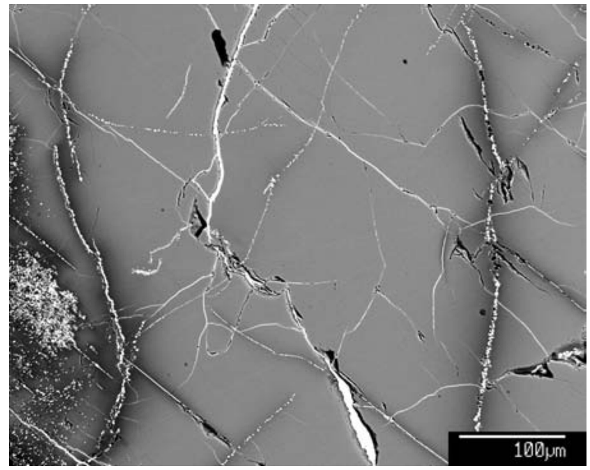

Fig. 2. Silicate darkening in a portion of a Fa13.8 olivine grain (light gray) in ALH 77257. The left edge of the grain is a reduction rim with numerous low-Ni metallic Fe blebs (white). Some curvilinear trails of metal blebs are flanked by dark-gray-shaded olivine of lower FeO content; these trails also seem to have formed by reduction. Many of the small opaque trails contain metal and rare sulfide grains; these trails formed by shock-injection of metal and sulfide into fractures in the olivine. The continuous white trails through the olivine are terrestrial weathering veins containing limonite. BSE image.

olivine, indicating that these are also reduction features. Reduction is a period 3 effect superimposed on the olivine grains after their initial shock.

On the other hand, some of the small curvilinear trails in the olivine grain were not produced by reduction. These trails are not flanked by low-FeO olivine, and some of these trails contain small grains of Fe sulfide, a phase that cannot form from olivine by reduction. These trails are characteristic of the shock feature known as silicate darkening. This feature is exactly analogous to silicate darkening in shocked ordinary chondrites (OC) and corresponds to shock stage ≥S3 (Rubin 1992). Silicate darkening is produced by shock-heating metal-sulfide above the Fe-FeS eutectic temperature (988 °C), mobilization of the melt, and incorporation of the melt into fractures within adjacent silicate grains.

Most ureilites contain olivine grains that exhibit undulose extinction and possess irregular fractures. This is consistent with shock-stage S2 (Stöffler et al. 1991) and indicates a shock pressure of <4–5 GPa (Stöffler et al. 1991; Schmitt et al. 1994; Schmitt and Stöffler 1995). Some ureilites (e.g., Northwest Africa [NWA] 1464, Elephant Moraine [EET] 90019, and PCA 82506) contain olivine with undulose extinction and planar fractures, consistent with shock stage S3 and corresponding to shock pressures of 5–10 GPa. Some ureilites exhibit fracturing, kinking, and translation gliding in silicate grains; these characteristics were probably also caused by shock processes (Berkley et al. 1980).

The C polymorphs diamond and lonsdaleite occur in the carbonaceous matrix of many ureilites (Lipschutz 1964). Haverö contains chaoite (C) along with diamond and lonsdaleite (Vdovykin 1972). Although Fukunaga et al. (1987) suggested that ureilite diamonds could have formed by growth in a vapor, the presence of lonsdaleite and chaoite strongly implies that all three carbon polymorphs were formed by shock (Vdovykin 1972). Shock pressures of at least 100 GPa appear to have been involved (Carter et al. 1968).

Fine-grained interstitial silicates consisting of magnesian low-Ca pyroxene, augite and Si-Al-alkali-rich glass occur in nearly all ureilites (Goodrich 1992). Compared to the cores of adjacent large silicate grains, the interstitial silicates are enriched in CaO, Al_2O_3, Na_2O, and K_2O (Goodrich 1986). In equilibrated chondrites, these elements are preferentially concentrated in plagioclase. They are also enriched in melt pockets in OC that formed in situ by shock melting (Dodd and Jarosewich 1979, 1982). The enrichment of the OC melt pockets in these "plagiophile" elements is due to preferential melting of plagioclase during shock events: plagioclase is a highly compressible phase that has a low impedance to shock compression (Schaal et al. 1979). Although plagioclase is essentially absent in monomict ureilites, it is common among clasts in polymict ureilites (Goodrich 1992). I suggest that the fine-grained silicates in ureilites are a plagiophile-element-rich shock product injected into these rocks during period 2 shock events.

Many ureilites contain a minor, heterogeneously distributed phase enriched in light rare earth elements (LREE) (Boynton et al. 1976; Spitz and Boynton 1986; Goodrich et al. 1987, 1991). It is present in some fractions of Kenna and RC027, but absent in others. The phase is soluble in HNO_3; the LREE-enriched leachate constitutes <50 mg/g of ureilites (Goodrich 1992). This LREE-rich phase may also be a shock product injected into ureilites during period 2.

Among the ureilites in this study, ~57% (16/28) appear to have remained unchanged after period 2 (Table 1).

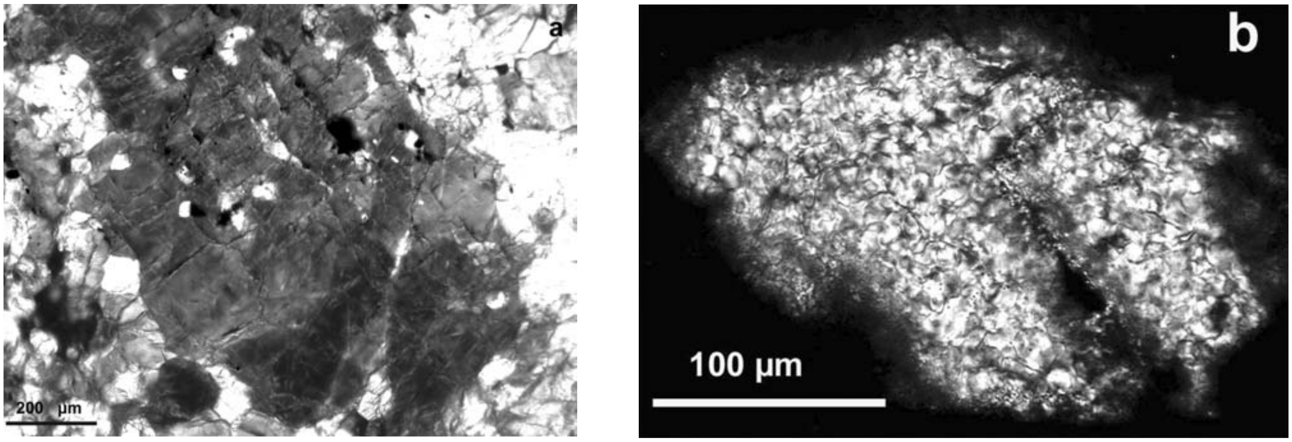

Fig. 3. Mosaicized olivine grains in ordinary chondrites. a) Mottled, mosaicized olivine grain in the shock stage S5 fall Alfianello (L6). The grain consists of small, poorly defined domains with slightly different extinction angles. X-nicols. b) Olivine aggregate embedded in the melt fraction of the Rose City H5 impact-melt breccia. The aggregate consists of small, individual unstrained olivine crystals and seems to have formed from a mosaicized olivine grain by annealing. X-nicols.

Period 3: Post-Shock Annealing

Coarse mosaicized olivine grains in shock-stage-S5 OC are characterized by a mottled appearance (Fig. 3a) when viewed in transmitted light under crossed polarizers (Carter et al. 1968; Reimold and Stöffler 1978). These coarse olivine grains consist of numerous, approximately equant, poorly defined domains, several micrometers across, that differ in their extinction positions by at least 3 to 5° (Stöffler et al. 1991).

Rubin (1995) described coarse olivine aggregates within the melt regions of the Chico and Rose City OC impact-melt breccias that appear to be mosaicized olivine grains (Fig. 3b) that were annealed by the surrounding silicate melt. The olivine aggregates contain numerous 10–20 µm, essentially unstrained individual faceted olivine crystals with 120° triple junctions.

Several ureilites contain analogous coarse olivine aggregates that are composed of numerous unstrained olivine crystals, many with 120° triple junctions (Figs. 4a–c). The small unstrained crystals within the olivine aggregates in EET 87720, Graves Nunataks (GRA) 95205, and Lewis Cliff (LEW) 86216 are ~20–40 µm in size; those in ALH 81101 are ~50–80 µm (Fig. 4c). Haverö contains similar olivine aggregates (Vdovykin 1976). Although the coarse olivine aggregates have been described simply as mosaicized grains (e.g., in ALH 81101; Table 1 of Goodrich 1992), they instead appear to be annealed mosaicized olivine aggregates analogous to those in the melt portions of the OC impact-melt breccias (Fig. 3b).

Bauer (1979) and Ashworth and Mallinson (1985) found that shock-induced damage of the olivine crystal lattice can be repaired during annealing at subsolidus temperatures, and it seems likely that annealing in ureilites is responsible for converting normal mosaicized olivine into olivine aggregates containing numerous individual unstrained crystals.

Bischoff et al. (1999) noted the annealed mosaicized olivine grains in some of these ureilites and ascribed their textures to recrystallization produced in shock stage S6 rocks. However, in view of the evidence for shock and annealing in ALH 81101 (see below), it seems likely that the unstrained mosaicized olivines were produced during annealing, not via recrystallization induced by very high shock pressures.

Verification of the annealing process is evident in ALH 81101. Some pigeonite grains in this meteorite contain planar fractures and exhibit pronounced undulose to weak mosaic extinction indicative of shock stage S3-S4. Some of these pigeonite grains enclose olivine aggregates composed of tiny individual unstrained olivine crystals (Fig. 4d). The enclosed olivine aggregates and surrounding pigeonite must have experienced identical shock pressures. However, because diffusion is much more rapid in olivine than in pyroxene (e.g., Freer 1981; Chakraborty 1997), annealing would have healed the damaged olivine crystal lattices prior to healing the pyroxene lattices. In ALH 81101, annealing ceased before pigeonite was significantly affected. Thus, the pigeonite preserves its shock features while the enclosed olivine grains were healed of the shock-induced damage to their crystal lattices.

Many ureilites possess coarse (silicate-darkened) olivine grains that contain curvilinear trails of small metallic Fe-Ni and sulfide blebs that are confined to the interiors of the grains (Figs. 2 and 5a). If the trails initially had been incorporated into fractures and the fractures are no longer evident, this suggests that annealing of the host caused the fractures to heal, sealing the opaque blebs inside.

Coarse olivine grains in ALH 84136 possess extensive reduction rims that extend from the edges of the grains (which are adjacent to carbonaceous material in the meteorite matrix) toward the grain centers (Goodrich 1992). In some cases, the reduction zones encompass the entire olivine grains; in others, the zones extend only one-third to one-half of the

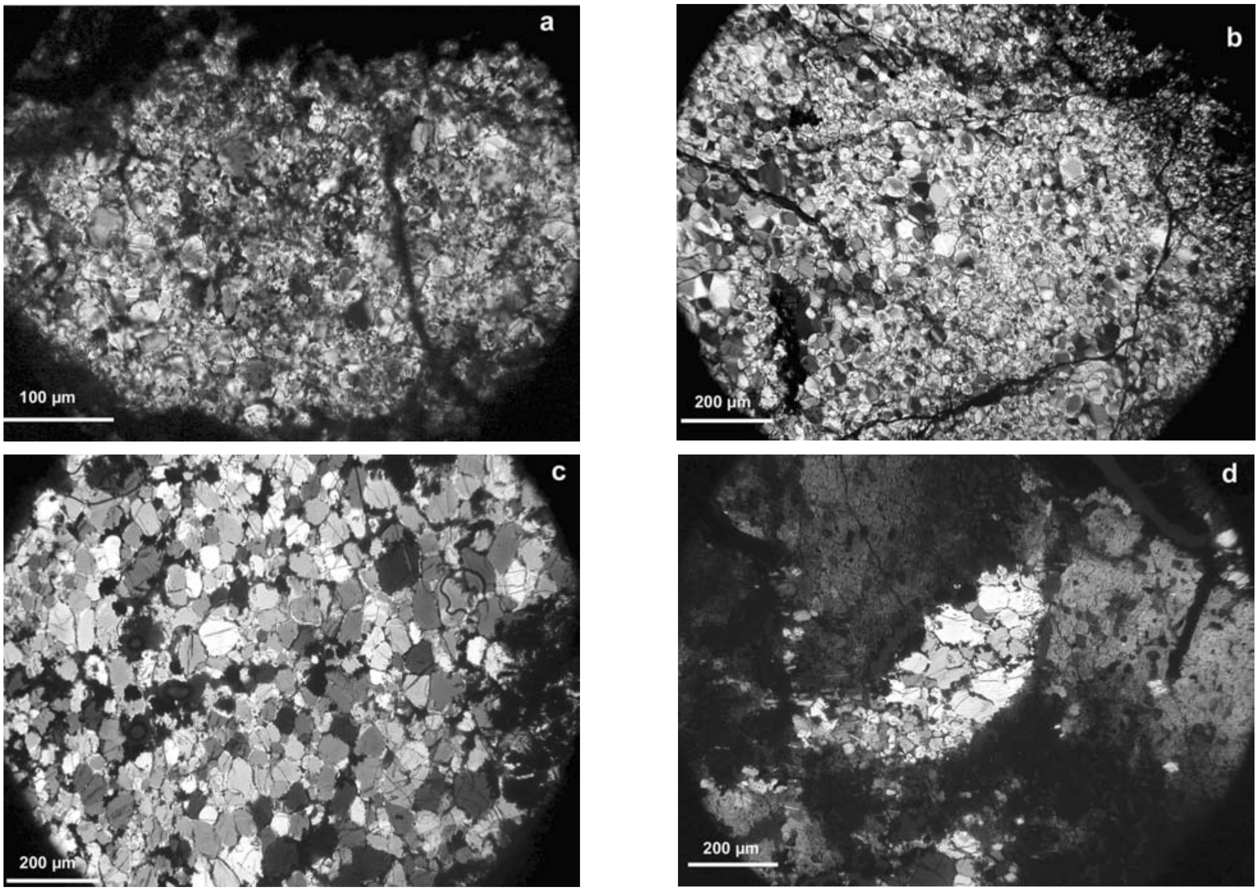

Fig. 4. Mosaicized olivine in ureilites. a) Olivine aggregate in EET 87720 formed from an annealed mosaicized olivine grain. Numerous relatively coarse individual unstrained crystals compose the aggregate. X-nicols. b) Olivine aggregate in GRA 95205 formed from an annealed mosaicized olivine grain. Numerous, randomly oriented, unstrained olivine crystals are evident. X-nicols. c) Numerous, moderately coarse unstrained olivine crystals with random orientations within a large olivine aggregate in ALH 81101. X-nicols. d) Small olivine aggregate (light gray; center) in ALH 81101 composed of unstrained individual olivine crystals. The aggregate formed from a mosaicized olivine grain. The aggregate is embedded within a large pigeonite grain with undulose extinction (dark to medium gray). X-nicols.

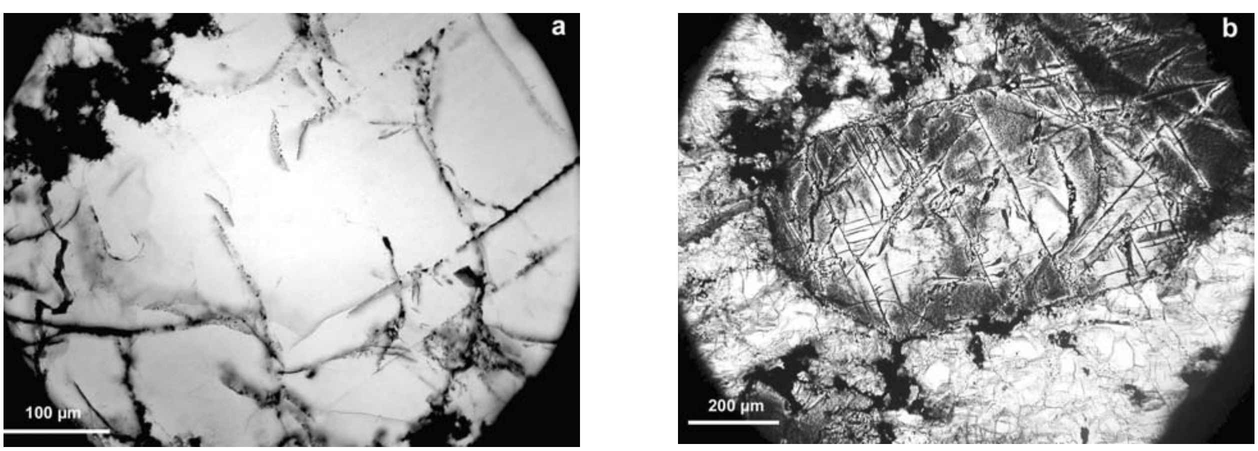

Fig. 5. By-products of annealing. a) Short curvilinear trails of tiny opaque blebs (black) sealed within healed fractures in an olivine grain (light gray) in Nova 001. Transmitted light. b) Reduction rims (dark, dusty regions) at the edges of an olivine grain (center) in ALH 84136. The reduced regions, which cover more than half of the grain, are composed of numerous tiny blebs of low-Ni metallic Fe. Transmitted light.

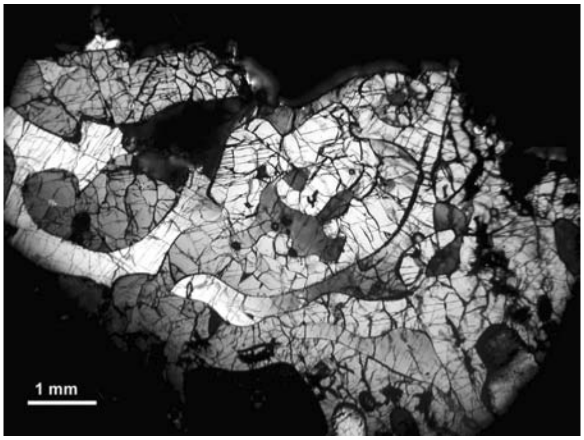

Fig. 6. Sinuous, quasi-granulitic texture of olivine and pyroxene grains in MET 78008. This is most likely a result of significant annealing. X-nicols.

distance from the edge of the grains to the center (e.g., Fig. 5b). The reduction zones, which appear dark in transmitted light, consist of thousands of tiny (0.1–1.0 μm) low-Ni metallic Fe blebs. It seems plausible that annealing facilitated the redox reaction between FeO in the olivine and C in the matrix. The simplest versions of this reaction are:

$$FeO + C \rightarrow Fe + CO$$

and

$$2FeO + C \rightarrow 2Fe + CO_2$$

A few ureilites (e.g., ALH 78019, ALH 83014, Nova 001) contain apparently euhedral graphite laths (up to 0.3 × 1 mm in size), some with pyramidal terminations, interstitial to coarse mafic silicate grains (Berkley and Jones 1982; Goodrich 1992; Treiman and Berkley 1994). Although the euhedral graphite grains could be a primary magmatic phase, this seems unlikely in a large magma body because the low density of graphite (2.23 g cm^{-3}) relative to that of ultramafic liquids (≥2.85 g cm^{-3}) would result in graphite flotation unless crystallization was rapid (as inferred for impact-melted enstatite chondrites) (e.g., Rubin 1997) or strong convection currents kept the magma well mixed. Alternatively, it is possible that the graphite laths crystallized in place within a cumulus pile or recrystallized from carbonaceous material in a body with only a small amount of melt (A. H. Treiman, personal communication). Another possibility is that the graphite laths are idioblastic (i.e., euhedral-appearing grains produced during metamorphism), having achieved their faceted shapes as a result of annealing. Minerals with high anisotropy such as graphite are more likely than less-anisotropic phases to form idioblastic shapes during thermal metamorphism (Spry 1969).

MET 78008 is a ureilite that can constrain the shock and annealing process. Preserved shock effects include silicate darkening and undulose extinction in low-Ca pyroxene. The meteorite does not contain abundant pigeonite. Instead, augite and orthopyroxene occur, with small amounts of pigeonite present as inclusions in the augite (Goodrich 1992). The clinopyroxene-orthopyroxene inversion temperature for FeO-bearing pyroxenes is on the order of 980 °C (Brown 1972), suggesting that MET 78008 was annealed at approximately this temperature. Annealing is also probably responsible for the sharp optical extinction of the olivine (characteristic of shock-stage S1). (The silicate darkening in this rock indicates that it had previously been shocked to at least shock stage S3.)

The texture of MET 78008 is unusual for a ureilite: elongated, sinuous olivine grains in MET 78008 wrap around low-Ca pyroxene grains (Fig. 6). Grain boundaries are smooth and curvy. The rock's texture resembles that of a granulite (e.g., Plate IXd of Spry 1969) or an amphibolite (Fig. 68b of Heinrich 1956).

The timing of the formation and annealing events for MET 78008 is constrained by the Rb-Sr model age of 4.55 Ga and the Rb-Sr internal isochron age of 4.01 ± 0.06 Ga (Takahashi and Matsuda 1990). Goodrich et al. (1991) reported a Sm-Nd whole-rock age of ~4.55 Ga for MET 78008, consistent with the Rb-Sr model age. It thus appears that MET 78008 formed 4.55 Ga ago and experienced closed-system metamorphism (i.e., annealing) ~4.0 Ga ago during a heating episode that did not disturb the Sm-Nd systematics (Goodrich 1992). The 4.0 Ga annealing event occurred 550 Ma after accretion. This is equivalent to ~750 half-lives of ^{26}Al (where $t_{1/2} = 0.73$ Ma), indicating that ^{26}Al decay could not have been responsible for the annealing. Impacts are the only plausible heat source at this late date.

Among the ureilites in this study, ~36% (10/28) experienced period 3 events, but remained unchanged afterward (Table 1).

Period 4: Post-Annealing Shock

EET 83309 is a polymict ureilite, a set that also includes North Haig, Nilpena, EET 87720, Frontier Mountain 90200 (and presumably paired specimens), Dar al Gani 319 (and 665), Dar al Gani 164 (and 165), and NWA 1926. EET 83309 is a regolith breccia containing a high concentration of solar wind–implanted ^{4}He (Ott et al. 1990). The rock is extensively brecciated; in addition to possessing the typical ureilite texture consisting of millimeter-size mafic silicate grains, it contains a finer-grained portion with 200 μm angular grains of olivine, twinned pigeonite, and annealed mosaicized olivine aggregates.

The brecciation and introduction of clasts into the polymict ureilites post-date the annealing of the mosaicized olivine grains and thus offer evidence of impact events that occurred after annealing. It is also probable that the ^{15}N-enriched component (with a composition of $\delta^{15}N \geq 600‰$) was introduced into the polymict ureilites during a late-stage brecciation event (Grady and Pillinger 1988).

There is direct petrographic evidence in EET 83309 of post-annealing shock. Some of the mosaicized olivine aggregates in EET 83309 are not unstrained (Fig. 7). The small faceted olivine crystals within some coarse mosaicized olivine aggregates exhibit undulose extinction (characteristic of shock-stage S2), indicating that the grains were (very weakly) shocked after annealing (The observation that the small olivine crystals within the aggregates are individual grains and not poorly defined domains indicates that the aggregates are not simply mosaicized olivine grains. Instead, they were formed from mosaicized olivine grains by sequential processes of annealing and shock.).

Other polymict ureilites (as well as the anomalous ureilite Larkman Nunatak [LAR] 04315) may also have experienced period 4 events; about 7% of ureilites seem to have reached this level. Suessite (Fe_3Si) in the North Haig polymict ureilite probably formed by shock-heating of kamacite and concomitant reduction of silicate (Keil et al. 1982). This phase may have been produced during a post-annealing shock event. Although EET 87720 is also a polymict ureilite and might have experienced period 4 events, our single available thin section does not show petrographic evidence of post-annealing shock.

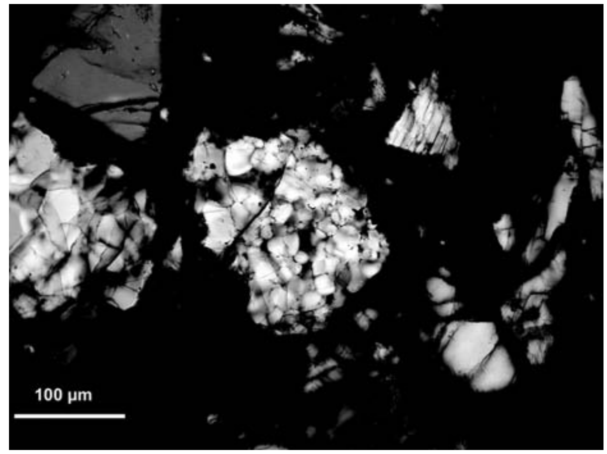

Fig. 7. Olivine aggregate in the clastic portion of the EET 83309 polymict breccia. The aggregate probably formed from a mosaicized olivine grain by annealing. Individual olivine crystals within the aggregate exhibit undulose extinction, indicating that the aggregate was shocked after it was annealed. X-nicols.

Implications for Ureilite Petrogenesis

Out of the four periods in ureilite history defined here, three (periods 2–4) involve impacts and impact heating. Collisions are directly responsible for the shock effects (e.g., Fig. 2) recorded in period 2 (e.g., silicate darkening; undulose extinction, planar fractures, and mosaicism in olivine; fracturing, kinking and translation gliding in silicate grains; and the production of diamond, lonsdaleite, and chaoite). Collisions are responsible for the annealing (Fig. 4) evident in period 3; MET 78008 was annealed 550 Ma after accretion when impacts were the only viable heat source. Collisions during period 4 are responsible for causing the development of undulose extinction in the small olivine crystals within the mosaicized olivine aggregates in the EET 83309 polymict ureilite (Fig. 7). Given the importance that collisions played in the history of ureilites, it is worthwhile to explore the possibility that collisions were also responsible for forming ureilites during period 1.

As suggested by Rubin (1988), impacts into an undifferentiated chondritic parent body with heterogeneous O isotopes (such as a CV chondrite–like body) could account for the principal O-isotopic properties of ureilites (Clayton and Mayeda 1988). Different ureilites (or, perhaps, different ureilite subgroups) may have formed in different cratering events. Primitive chondritic characteristics that survived ureilite melting include the oxidation state (as reflected in olivine Fa) and the bulk Ir concentration. Both properties correlate with O-isotopic composition (Figs. 2 and 4 of Clayton and Mayeda 1988).

High concentrations of planetary-type noble gases are present in chondrites, but not in basaltic achondrites (e.g., Hintenberger et al. 1969; Bogard et al. 1971; Begemann et al. 1976). The high concentrations of planetary-type noble gases in ureilites (Stauffer 1961; Mazor et al. 1970; Weber et al. 1971; Bogard et al. 1973; Wilkening and Marti 1976; Gobel et al. 1978; Wacker 1986) are consistent with very brief heating episodes and rapid burial minimizing the time available for noble gases to escape.

Among siderophile trace elements in ureilites, refractory siderophile elements (W, Re, Os, and Ir) have abundances ranging from ~0.1 to 2.2 × CI, whereas common and volatile siderophile elements (Co, Ni, Ga, Ge, and Au) have lower abundances (~0.07 to 0.7 × CI) (Goodrich 1992). In contrast, these elements have much lower abundances in ultramafic rocks from the Earth, Moon, and Mars (typically 0.002 to 0.01 × CI) (Fig. 9 of Goodrich 1992). The relatively high concentrations of siderophile elements in ureilites are inconsistent with large-scale melting and differentiation. They are more consistent with a model involving impact melting, rapid cooling, and incomplete separation of metal from silicate.

The major arguments for an evolved, igneous origin of ureilites can also be broadly accounted for by an impact-melting model:

The occurrence of numerous plagioclase-rich clasts in polymict ureilites indicates that plagioclase was indeed present on the parent body when ureilites formed. When coupled with the relatively high concentrations of siderophile elements in ureilites, this suggests that the initial mineralogy of ureilites (or ureilite precursors) was basically chondritic, dominated by olivine, pyroxene, plagioclase, and metal. The virtual absence of plagioclase in the monomict ureilites may be due to the preferential melting and mobilization of plagioclase during collisional heating caused by the low impedance of this phase to shock compression. Loss of plagioclase accounts for the low abundances in the monomict ureilites of such moderately volatile “plagiophile” elements as K and Rb. It also accounts for low Al in ureilites (because Al was lost along with the plagioclase) and, consequently, the high bulk Ca/Al ratios of these rocks.

Low concentrations of other volatile elements (e.g., In, Cs, and Bi) in many ureilites (e.g., Goodrich 1992) could be due to volatilization during impact heating. Such volatile trace elements are also depleted in thermally metamorphosed OC (Dodd et al. 1967; Wood 1967; Dodd 1969; Wasson 1972).

The preferred alignment of elongated olivine and pyroxene crystals in ureilites (e.g., Kenna) (Figs. 1b and 1c of Berkley et al. 1976) may reflect settling of these grains to the floor of the crater at the base of the impact-melt pool. Alternatively, the petrofabrics could have resulted from shock-induced deformation as in CV, OC, and CR chondrites (e.g., Cain et al. 1986; Sneyd et al. 1988; Weisberg et al. 1993).

Ureilites probably formed with a LREE-depleted rare-earth pattern, reflecting the basic olivine-pyroxene mineralogy of these rocks (olivine is low in REE and has a relatively flat pattern; low-Ca pyroxene has higher concentrations of REE and is appreciably depleted in LREE [e.g., Zielinski 1975]) The common V-shaped REE pattern in ureilites may have been produced after a minor LREE-rich component was injected into many ureilites during period 2 events.

Impact-melting processes seem best able to account for the petrogenesis of ureilites. After formation, additional collisions caused shock effects and annealing episodes. Successive impact events are responsible for the myriad textural and compositional properties of this enigmatic group.

Acknowledgments–I thank P. H. Warren for sharing the ureilite thin sections in his care. I am grateful to the curators at NASA-Johnson Space Center and the American Museum of Natural History, as well as to A. H. Treiman of the Lunar and Planetary Institute for the loan of additional thin sections. The manuscript benefited from the reviews of Y. Ikeda and S. J. Singletary and the comments of associate editor A. H. Treiman. This work was supported by NASA Grant No. NAG5-4766.

Editorial Handling—Dr. Allan Treiman

REFERENCES

Ashworth J. R. and Mallinson L. G. 1985. Transmission electron microscopy of L-group chondrites, 2. Experimentally annealed Kyushu. *Earth and Planetary Science Letters* 73:33–40.

Bauer J. F. 1979. Experimental shock metamorphism of mono- and polycrystalline olivine: A comparative study. Proceedings, 10th Lunar and Planetary Science Conference. pp. 2573–2596.

Begemann F., Weber H. W., Vilcsek E., and Hintenberger H. 1976. Rare gases and ^{36}Cl in stony-iron meteorites: Cosmogenic elemental production rates, exposure ages, diffusion losses and thermal histories. *Geochimica et Cosmochimica Acta* 40:353–368.

Berkley J. L. 1986. Four Antarctic ureilites: Petrology and observations on ureilite petrogenesis. *Meteoritics* 21:169–187.

Berkley J. L., Brown H. G., Keil K., Carter N. L., Mercier J.-C. C., and Huss G. 1976. The Kenna ureilite: An ultramafic rock with evidence for igneous, metamorphic, and shock origin. *Geochimica et Cosmochimica Acta* 40:1429–1437.

Berkley J. L. and Jones J. H. 1982. Primary igneous carbon in ureilites: Petrological implications. Procedings, 13th Lunar and Planetary Science Conference. pp. A353–A364.

Berkley J. L., Taylor G. J., Keil K., Harlow G. E., and Prinz M. 1980. The nature and origin of ureilites. *Geochimica et Cosmochimica Acta* 44:1579–1597.

Bischoff A., Goodrich C. A., and Grund T. 1999. Shock-induced origin of diamonds in ureilites (abstract #1100). 30th Lunar and Planetary Science Conference. CD-ROM.

Bogard D. D., Gibson E. K., Moore D. R., Turner N. L., and Wilkin R. B. 1973. Noble gases and carbon abundances of the Haverö, Dingo Pup Donga, and North Haig ureilites. *Geochimica et Cosmochimica Acta* 37:547–557.

Bogard D. D., Huneke J. C., Burnett D. S., and Wasserburg G. J. 1971. Xe and Kr analysis of silicate inclusions from iron meteorites. *Geochimica et Cosmochimica Acta* 35:1231–1254.

Boynton W. V., Starzyk P. M., and Schmitt R. A. 1976. Chemical evidence for the genesis of the ureilites, the achondrite Chassigny and the nakhlites. *Geochimica et Cosmochimica Acta* 40:1439–1447.

Brown G. M. 1972. Pigeonitic pyroxenes: A review. *Geological Society of America Memoir* #132. pp. 523–534.

Cain P. M., McSween H. Y., and Woodward N. B. 1986. Structural deformation of the Leoville chondrite. *Earth and Planetary Science Letters* 77:165–175.

Carter N. L., Raleigh C. B., and Decarli P. S. 1968. Deformation of olivine in stony meteorites. *Journal of Geophysical Research* 73: 5439–5461.

Chakraborty S. 1997. Rates and mechanisms of Fe-Mg interdiffusion in olivine at 980–1300 °C. *Journal of Geophysical Research* 102: 12,317–12,331.

Clayton R. N. and Mayeda T. K. 1988. Formation of ureilites by nebular processes. *Geochimica et Cosmochimica Acta* 52:1313–1318.

Dodd R. T. 1969. Metamorphism of the ordinary chondrites: A review. *Geochimica et Cosmochimica Acta* 33:161–203.

Dodd R. T. and Jarosewich E. 1979. Incipient melting and shock classification of L-group chondrites. *Earth and Planetary Science Letters* 44:335–340.

Dodd R. T. and Jarosewich E. 1982. The compositions of incipient shock melts in L6 chondrites. *Earth and Planetary Science Letters* 59:355–363.

Dodd R. T., van Schmus W. R., and Koffman D. M. 1967. A survey of the unequilibrated ordinary chondrites. *Geochimica et Cosmochimica Acta* 31:921–951.

Freer R. 1981. Diffusion in silicate minerals and glasses: A data digest and guide to the literature. *Contributions to Mineralogy and Petrology* 76:440–454.

Fukunaga K., Matsuda J., Nagao K., Miyamoto M., and Ito K. 1987. Noble-gas enrichment in vapour-growth diamonds and the origin of diamonds in ureilites. *Nature* 328:141–143.

Gobel R., Ott U., and Begemann F. 1978. On the trapped noble gases in ureilites. *Journal of Geophysical Research* 83:855–867.

Goodrich C. A. 1986. Trapped primary silicate liquid in ureilites (abstract). 17th Lunar and Planetary Science Conference. pp. 273–274.

Goodrich C. A. 1992. Ureilites: A critical review. *Meteoritics* 27: 327–352.

Goodrich C. A. and Berkley J. L. 1986. Primary magmatic carbon in ureilites: Evidence from cohenite-bearing metallic spherules. *Geochimica et Cosmochimica Acta* 50:681–691.

Goodrich C. A., Jones J. H., and Berkley J. L. 1987. Origin and evolution of the ureilite parent magmas: Multi-stage igneous activity on a large parent body. *Geochimica et Cosmochimica Acta* 51:2255–2273.

Goodrich C. A., Patchett P. J., Lugmair G. W., and Drake M. J. 1991. Sm-Nd and Rb-Sr isotopic systematics of ureilites. *Geochimica et Cosmochimica Acta* 55:829–848.

Grady M. M. and Pillinger C. T. 1988. ^{15}N-enriched nitrogen in polymict ureilites and its bearing on their formation. *Nature* 331: 321–323.

Heinrich E. W. 1956. *Microscopic petrography*. New York: McGraw-Hill Book Co. 296 p.

Hintenberger H., Schultz L., and Weber H. 1969. Rare gases in the iron and in the inclusions of the Campo del Cielo meteorite, El Taco. In *Meteorite Research*, edited by Millman P. M. Dordrecht: Reidel. pp. 895–900.

Hutchison R. 2004. *Meteorites: A petrologic, chemical and isotopic synthesis*. Cambridge: Cambridge University Press. 506 p.

Keil K., Berkley J. L., and Fuchs L. 1982. Suessite, Fe_3Si: A new mineral in the North Haig ureilite. *American Mineralogist* 67: 126–131.

Lipschutz M. E. 1964. Origin of diamonds in the ureilites. *Science* 143:1431–1434.

Mazor E., Heymann D., and Anders E. 1970. Noble gases in carbonaceous chondrites. *Geochimica et Cosmochimica Acta* 34: 781–824.

Ott U., Löhr H. P., and Begemann F. 1990. EET 83309: A ureilite with solar noble gases (abstract). *Meteoritics* 25:396.

Reimold W. U. and Stöffler D. 1978. Experimental shock metamorphism of dunite. Proceedings, 9th Lunar and Planetary Science Conference. pp. 2805–2824.

Rubin A. E. 1988. Formation of ureilites by impact-melting of carbonaceous chondritic material. *Meteoritics* 23:333–337.

Rubin A. E. 1992. A shock-metamorphic model for silicate darkening and compositionally variable plagioclase in CK and ordinary chondrites. *Geochimica et Cosmochimica Acta* 56:1705–1714.

Rubin A. E. 1995. Petrologic evidence for collisional heating of chondritic asteroids. *Icarus* 113:156–167.

Rubin A. E. 1997. Igneous graphite in enstatite chondrites. *Mineralogical Magazine* 61:699–703.

Schaal R. B., Hörz F., Thompson T. D., and Bauer J. F. 1979. Shock metamorphism of granulated lunar basalt. Proceedings, 10th Lunar and Planetary Science Conference. pp. 2547–2571.

Schmitt R. T., Deutsch A., and Stöffler D. 1994. Shock recovery experiments with the H6 chondrite Kernouve at preshock temperatures of 293 and 920 K (abstract). *Meteoritics* 29:529–530.

Schmitt R. T. and Stöffler D. 1995. Classification of chondrites (abstract). *Meteoritics* 30:574–575.

Scott E. R. D., Taylor G. J., and Keil K. 1993. Origin of ureilite meteorites and implications for planetary accretion. *Geophysical Research Letters* 20:415–418.

Singletary S. J. and Grove T. L. 2003. Early petrologic processes on the ureilite parent body. *Meteoritics & Planetary Science* 38:95–108.

Sneyd D. S., McSween H. Y., Sugiura N., Strangway D. W., and Nord G. L. 1988. Origin of petrofabrics and magnetic anisotropy in ordinary chondrites. *Meteoritics* 23:139–149.

Spitz A. and Boynton W. V. 1986. The light rare earth element host phase in ureilite meteorites (abstract). *Meteoritics* 21:515–516.

Spry A. 1969. *Metamorphic textures*. Oxford: Pergamon. 350 p.

Stauffer H. 1961. Primordial argon and neon in carbonaceous chondrites and ureilites. *Geochimica et Cosmochimica Acta* 24: 70–82.

Stöffler D., Keil K., and Scott E. R. D. 1991. Shock metamorphism of ordinary chondrites. *Geochimica et Cosmochimica Acta* 55: 3845–3867.

Takahashi K. and Matsuda A. 1990. The Rb-Sr and Sm-Nd dating and REE measurements of ureilites (abstract). *Meteoritics* 25:413.

Takeda H. 1987. Mineralogy of Antarctic ureilites and a working hypothesis for their origin and evolution. *Earth and Planetary Science Letters* 81:358–370.

Takeda H. 1989. Mineralogy of coexisting pyroxenes in magnesian ureilites and their formation conditions. *Earth and Planetary Science Letters* 93:181–194.

Takeda H., Mori H., and Ogata H. 1988. On the pairing of Antarctic ureilites with reference to their parent body. *Proceedings of the NIPR Symposium on Antarctic Meteorites*. National Institute of Polar Research. 1:145–172.

Takeda H., Mori H., Yanai K., and Shiraishi K. 1980. Mineralogical examination of the Allan hills achondrites and their bearing on the parent bodies. *Proceedings of the Fifth Symposium on Antarctic Meteorites*. National Institute of Polar Research Special Issue. 17:119–144.

Takeda H. and Yanai K. 1978. A thought on the ureilite parent body as inferred from pyroxenes in Yamato-74659. Proceedings, 11th Lunar and Planetary Science Symposium. Institute of Space and Aeronautical Science, University of Tokyo. pp. 189–194.

Treiman A. H. and Berkley J. L. 1994. Igneous petrology of the new ureilites Nova 001 and Nullarbor 010. *Meteoritics* 29:843–848.

Vdovykin G. P. 1972. Forms of carbon in the new Haverö ureilite of Finland. *Meteoritics* 7:547–552.

Vdovykin G. P. 1976. The Haverö meteorite. *Space Science Reviews* 18:749–776.

Wacker J. F. 1986. Noble gases in the diamond-free ureilite, ALHA 78019: The roles of shock and nebular processes. *Geochimica et Cosmochimica Acta* 50:633–642.

Warren P. H. and Kallemeyn G. W. 1989. Geochemistry of polymict ureilite EET83309, and a partially-disruptive impact model for ureilite origin. *Meteoritics* 24:233–246.

Warren P. H. and Kallemeyn G. W. 1992. Ureilites: The graphite f(O2) buffer, explosive volcanism, and the gross dissipation of basalt from the parent asteroid(s) (abstract). *Abstracts of the Lunar and Planetary Science Conference* 23:1497–1498.

Wasson J. T. 1972. Formation of ordinary chondrites. *Reviews of Geophysics and Space Physics* 10:711–759.

Weber H. W., Hintenberger H., and Begemann F. 1971. Noble gases in the Haverö ureilite. *Earth and Planetary Science Letters* 13: 205–209.

Weisberg M. K., Prinz M., Clayton R. N., and Mayeda T. K. 1993. The CR (Renazzo-type) carbonaceous chondrite group and its implications. *Geochimica et Cosmochimica Acta* 57:1567–1586.

Wilkening L. L. and Marti K. 1976. Rare gases and fossil particle tracks in the Kenna ureilite. *Geochimica et Cosmochimica Acta* 40:1465–1473.

Wood J. A. 1967. Chondrites: Their metallic minerals, thermal histories, and parent planets. *Icarus* 6:1–49.

Zielinski R. A. 1975. Trace element evaluation of a suite of rocks from Reunion Island, Indian Ocean. *Geochimica et Cosmochimica Acta* 39:713–734.